



ELSEVIER

Electron cryomicroscopy of single particles at subnanometer resolution

Wen Jiang and Steven J Ludtke

Electron cryomicroscopy and single-particle reconstruction have advanced substantially over the past two decades. There are now numerous examples of structures that have been solved using this technique to better than 10 Å resolution. At such resolutions, direct identification of α helices is possible and, often, β -sheet-containing regions can be identified. The most numerous subnanometer resolution structures are the icosahedral viruses, as higher resolution is easier to achieve with higher symmetry. Important non-icosahedral structures solved to subnanometer resolution include several ribosome structures, clathrin assemblies and, most recently, the Ca^{2+} release channel. There is now hope that, in the next few years, this technique will achieve resolutions approaching 4 Å, permitting a complete trace of the protein backbone without reference to a crystal structure.

Addresses

National Center for Macromolecular Imaging, Verna and Marrs McLean Department of Biochemistry and Molecular Biology, Baylor College of Medicine, Houston, TX 77030, USA

Corresponding author: Ludtke, Steven J (sludtke@bcm.tmc.edu)

Current Opinion in Structural Biology 2005, **15**:571–577

This review comes from a themed issue on
Biophysical methods
Edited by Wah Chiu and Keith Moffat

Available online 2nd September 2005

0959-440X/\$ – see front matter
© 2005 Elsevier Ltd. All rights reserved.

DOI 10.1016/j.sbi.2005.08.004

Introduction

The field of electron cryomicroscopy (cryo-EM) and, in particular, single-particle reconstruction has undergone dramatic growth in recent years (Figure 1). A combination of improvements in transmission electron microscope technology and rapid growth of computational capabilities has allowed this field to advance from achieving 30–40 Å resolution ten to fifteen years ago to now, when numerous structures at subnanometer resolution have been elucidated. At such resolutions, it is possible to directly determine the arrangement of secondary structure elements within three-dimensional reconstructions. As the field approaches 4–5 Å resolution, the goal of tracing the protein backbone solely from a single-particle reconstruction is on the verge of becoming a reality.

Single-particle reconstructions are generally divided into two categories: icosahedral particles and non-icosahedral particles. Typically, the resolution-limiting factor in single-particle reconstruction is the high noise levels present in the particle images due to dose limitations. As resolution increases, ever smaller doses are required to prevent radiation damage at the resolution of interest. In addition, specimen motion, beam coherence and other factors may limit the final resolution achievable for a given set of images. The most commonly studied icosahedral particles are large virus capsids, with masses sometimes exceeding 100 megadaltons. Combined with 60-fold symmetry, the effective signal to noise ratio of these particles is substantially higher than that of asymmetric particles, with masses typically measured in the hundreds of kilodaltons. In addition, the 60-fold symmetry reduces the number of particles required for a reconstruction at a given resolution by a factor of 60, permitting subnanometer resolution reconstructions to be performed using only a few thousand particles. Not surprisingly, the first structure solved at subnanometer resolution [1,2] was an icosahedral virus.

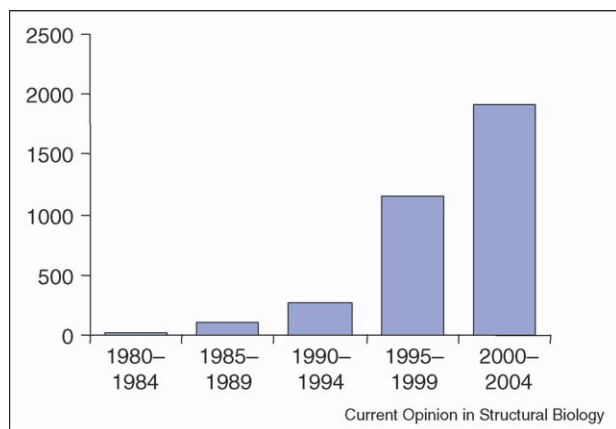
In this review, we survey subnanometer resolution reconstructions published to date. As these reconstructions are biologically diverse, the discussion is organized by the symmetry of the particle being discussed, starting with large icosahedral particles and gradually moving to lower symmetry particles.

Icosahedral viruses

Since achieving the subnanometer resolution milestone for the small hepatitis B virus core [1,2], the number of virus structures solved at this resolution has been steadily increasing. In fact, it is now possible to solve a virus structure from imaging to reconstruction and identification of secondary structure elements in well under a month. Although this throughput is still highly specimen dependent, it is beginning to transform cryo-EM into a routine laboratory technique, like cloning or gel filtration, for studying the structural and functional relationships of biological systems under various biochemical conditions or in various functional states.

Viruses from many different families have now been solved at subnanometer resolution: the small hepatitis B virus [1,2] and rhinovirus [3*] (~300 Å); the large adenovirus [4,5] (~930 Å) and herpes simplex virus [6] (~1250 Å); single-layered cytoplasmic polyhedrosis virus (CPV) [7]; multi-layered rice dwarf virus (RDV) [8] and reovirus [9**]; enveloped alphaviruses [10], dengue virus [11] and PM2 phage [12]; phages with a large non-icosahedral tail, such as

Figure 1



Growth of the cryo-EM field based on the number of publications identified using a Google Scholar search (with key words cryomicroscopy, cryoem and cryo-electron).

P22 [13^{••},14^{••}] and ϕ 29 [14^{••}]; and complexes of rhinovirus with cellular receptors [3[•]]. From these structures, significant insights into viral assembly, maturation and evolution have been achieved.

Identification of viral protein folds

Structures determined at subnanometer resolution allow assignment of secondary structure elements within the reconstruction, which can then be used to establish protein folds. The hepatitis B virus core [1,2], herpes simplex virus capsid [6] and RDV capsid [8] are reconstructions for which secondary structure elements and protein folds were first proposed based on cryo-EM structures and later confirmed using X-ray crystallography [15,16[•],17]. These successful cross-validations demonstrated that single-particle cryo-EM at subnanometer resolution provides accurate, biologically relevant structural information.

Evolutionary links among distinct viral families

The structure of the mature P22 phage at 9.5 Å resolution [13^{••}] revealed, for the first time, that the coat protein of a short-tailed phage, P22, shares the same fold as that of a long-tailed phage, HK97, despite minimal sequence identity (Figure 2a,b). This led to the hypothesis that the major coat proteins of most of the tailed phages share the same protein fold and thus possibly a common ancestor. This concept is further supported by the recent publication of the structure of the ϕ 29 phage capsid at 7.9 Å resolution [14^{••}] (Figure 2c), the capsid structure of ϵ 15 phage at 9.5 Å (W Jiang *et al.*, unpublished) and the crystal structure of isolated T4 vertex protein gp24 [18]. Surprisingly, the same fold has also been discovered in the floor domain of human herpes simplex virus (M Baker, W Jiang *et al.*, unpublished).

These findings are reshaping our understanding of the evolutionary relationships among virus families. The

well-known jelly-roll fold shared by small viruses [19], the conserved major coat proteins of double-stranded (ds)DNA adenoviruses, PRD1 phage and archaeal *Sulfolobus* turreted icosahedral virus [20], and the inner 'T = 2' shell proteins of dsRNA reovirus [21], CPV [7], RDV [8], bluetongue virus [22] and L-A virus [23] together raise the possibility that all viruses might have evolved from a relatively small number of primordial progenitors.

Structural dynamics

A distinct advantage of single-particle analysis is the capability to solve the structures of macromolecules in different functional states. The structures of several viruses, such as herpes simplex virus [24] and HK97 phage [25], have been studied in various functional states at lower resolution. Structures representing the transition of the P22 phage from procapsid to mature phage have been solved to 8.5 Å and 9.5 Å resolution, respectively [13^{••}]. These structures revealed the hinge motion of helices and sheets, and local refolding of one helix. These local conformational changes result in the large-scale expansion and angularization of the entire capsid, a signature of the maturation process of tailed phages.

Although not a virus, the E2 core of pyruvate dehydrogenase from *Bacillus stearothermophilus* has icosahedral symmetry. Several laboratories have studied this structure using both cryo-EM and X-ray crystallography. Two [26,27] have provided single-particle reconstructions at subnanometer resolution. One report [26] is of more technical than biological interest, as it was intended as a control for the development and evaluation of a new single-particle reconstruction methodology fundamentally different from that used for icosahedral virus particles.

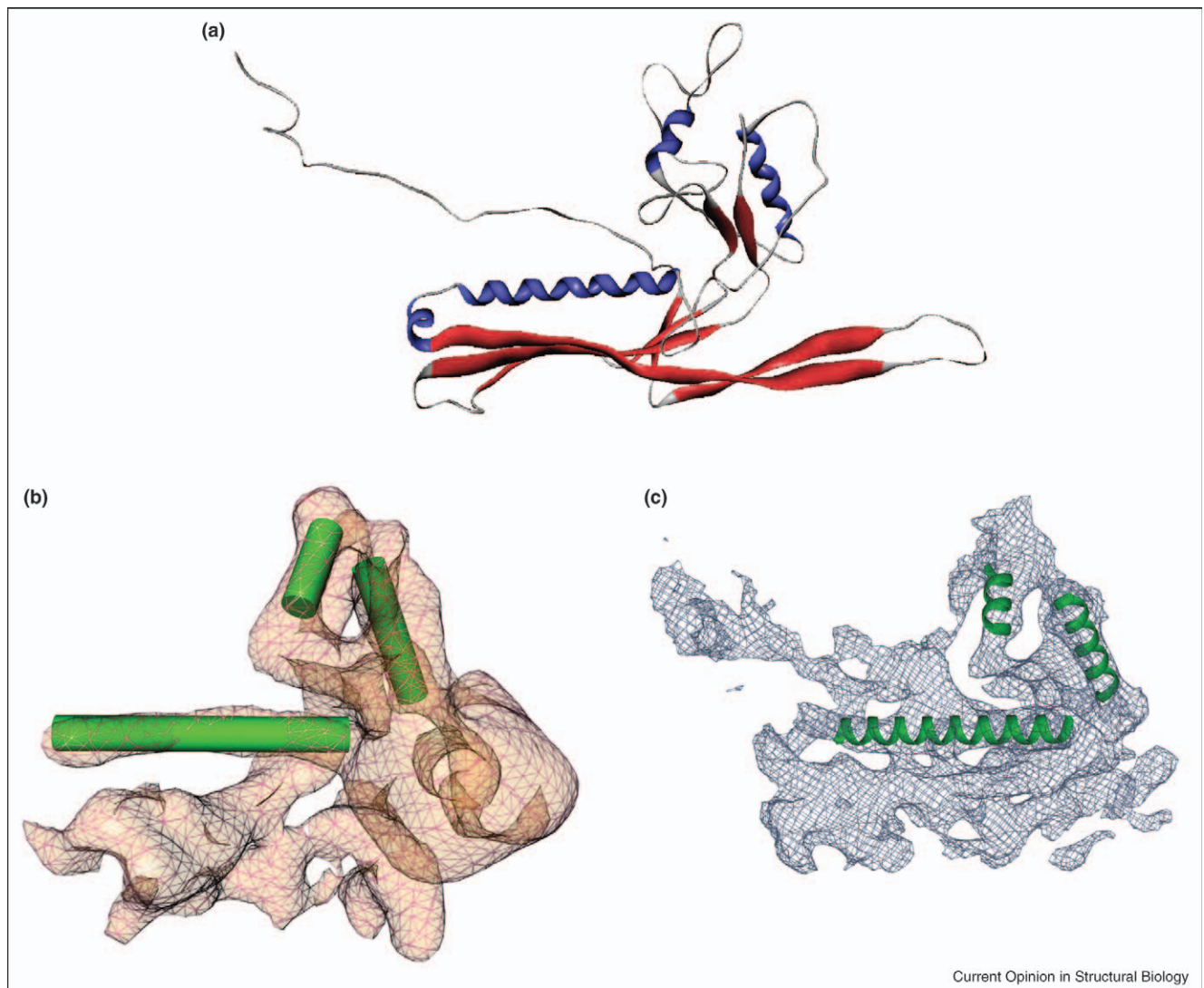
Structures with lower symmetry

The number of lower symmetry particles solved at subnanometer resolution is much more limited and the solved structures are far more biologically diverse. We begin with the higher symmetry reconstructions and then consider progressively lower symmetries.

Clathrin can form assemblies with a variety of symmetries. The structure of the D6 hexagonal barrel form of clathrin was recently solved at ~12 Å, which was then extended to ~8 Å resolution [28^{••}] through the use of additional subunit averaging beyond the D6 symmetry. α -Helical motifs can be clearly observed in the structure (Figure 3), making a convincing argument for true subnanometer resolution. This structure, combined with a moderately lower resolution reconstruction of mini-coats, provides some clues to how clathrin can form such diverse assemblies using fundamentally the same structural linkages.

GroEL (~800 kDa) represents an assembly that, despite the existence of several crystal structures, is still under active study using single-particle reconstruction. These

Figure 2



Comparison of tailed dsDNA phage major capsid shell proteins. **(a)** Single subunit of the crystal structure of HK97 phage capsid, **(b)** cryo-EM structure of P22 phage capsid and **(c)** cryo-EM structure of ϕ 29 phage capsid displayed in approximately the same orientation. The dispositions of helices and sheets are similar among these proteins. The common shell protein fold shared by these phages with negligible sequence homology suggests that these phages are evolutionally linked and could have evolved from a common ancestor. Panel (c) reproduced with permission from [14**].

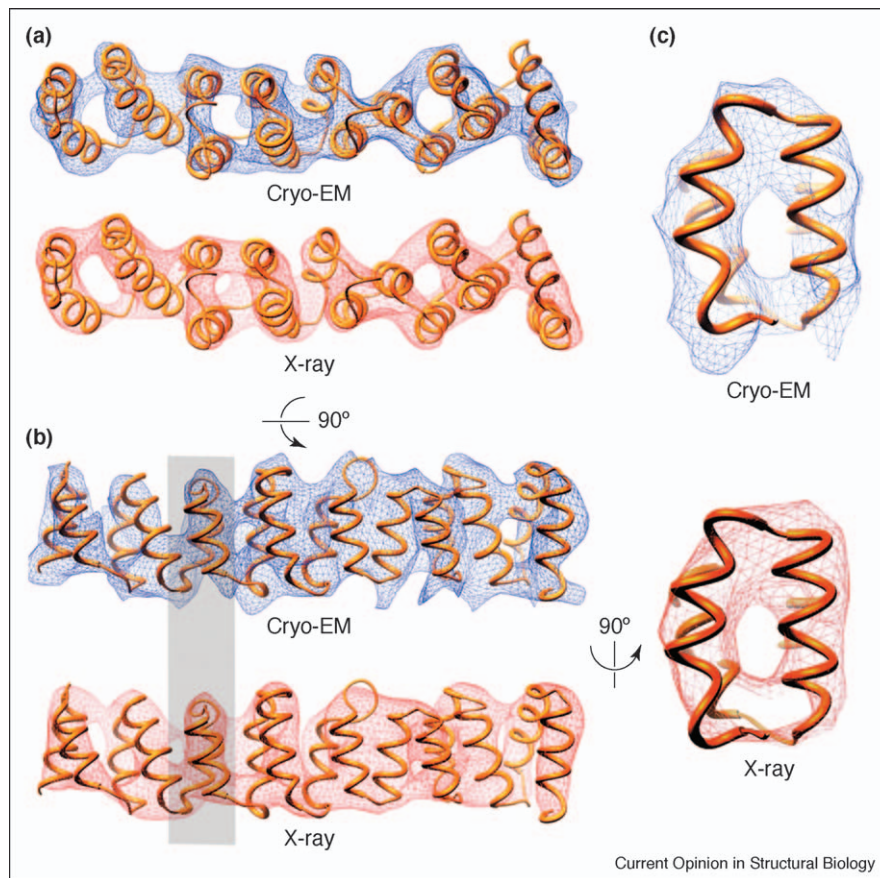
studies focus largely on functional states [29] and substrate binding, but have also demonstrated differences between the crystal structure and the cryo-EM structure of the solution state. The 6 Å resolution structure of native unliganded GroEL with 14-fold symmetry also represents the highest resolution single-particle reconstruction published to date [30**] (Figure 4).

In addition to the icosahedral shells discussed above, viral particles also contain non-icosahedral components, such as the genome, the polymerase of dsRNA viruses, the tail and connector of phages, and so on. The structures of isolated connectors from phages SPP1 (~750 kDa) [31*

and T7 (~710 kDa) [32*] have been solved at subnanometer resolution; the fold and 12-fold symmetry of these particles are related to that of the ϕ 29 connector crystal structure [33]. With the great successes in solving the icosahedral shells of many viruses at subnanometer resolution, attempts have been made to study these non-icosahedral components in association with the capsid [9**,34*,35], although with limited success.

The structure of the transferrin–transferrin receptor complex [36] represents the smallest structure yet solved at subnanometer resolution (~290 kDa). Both small size and lack of symmetry increase the difficulty of performing

Figure 3



Comparison of a portion of the subnanometer single-particle reconstruction of the clathrin lattice with the corresponding crystal structure. The atomic model is docked into the single-particle reconstruction (blue) and into density based on the crystal structure blurred to a similar resolution (red). **(a)** Top and **(b)** side views of the structure; **(c)** focuses on the set of helices shown in grey in **(b)**, demonstrating that they are clearly resolved. Reproduced with permission from [28**].

single-particle reconstructions, particularly at higher resolution. To obtain sufficient contrast when imaging smaller particles, images must generally be collected relatively far from focus, limiting the resolution of the raw data.

Among the best-known systems studied using single-particle reconstruction is the ribosome, with a variety of assemblies studied in various functional states. Only three of these reconstructions claim subnanometer resolution [37–39]. Despite their different resolution claims, empirically the resolution of these structures can be judged to be roughly equivalent. In general, the study of ribosomes and other structures that interact with or contain nucleic acids has an additional advantage over the study of pure protein structures. For proteins, subnanometer resolution is required to begin to identify secondary structure, whereas for DNA and RNA, helices can be observed in the 10–15 Å resolution range.

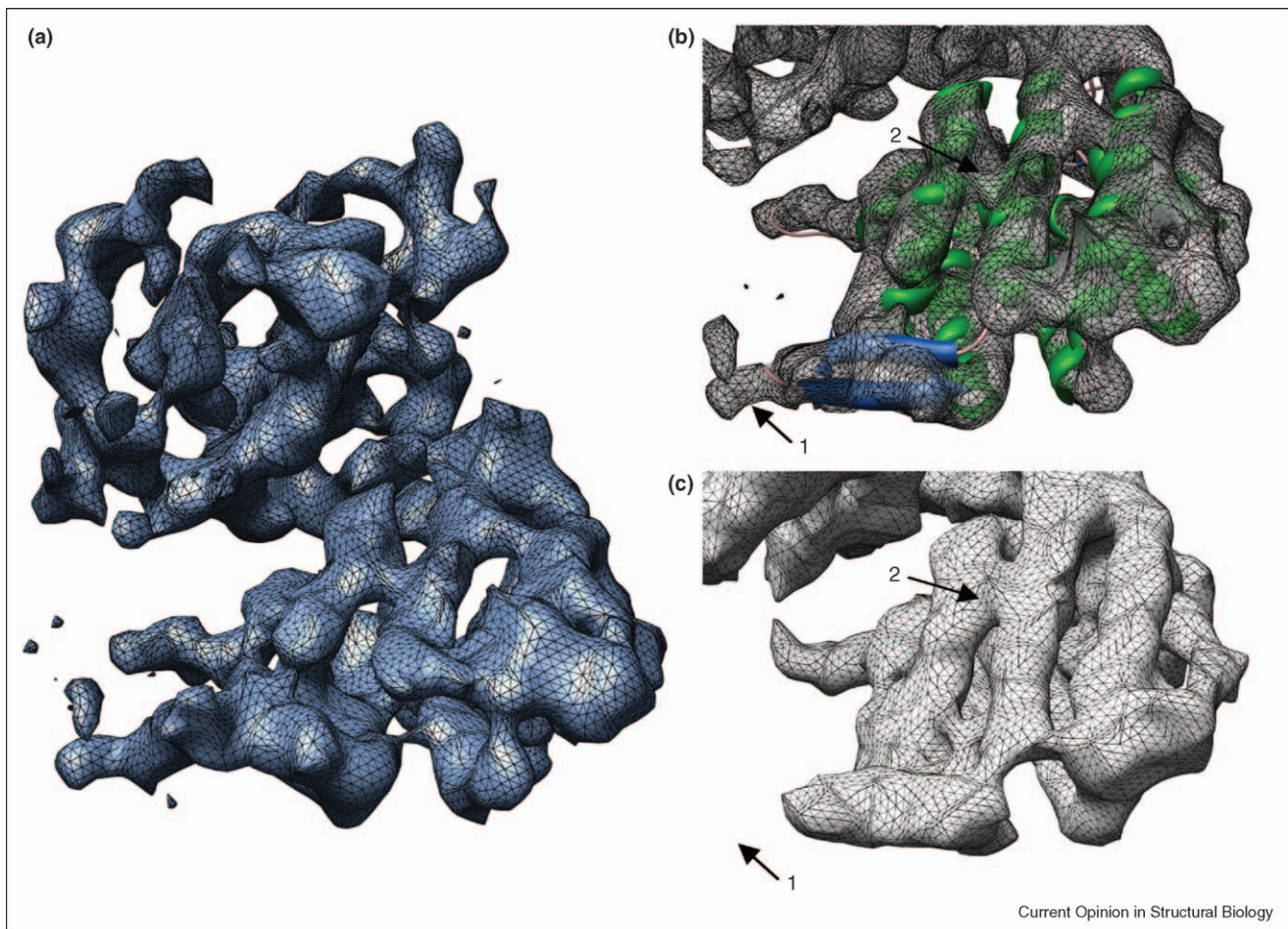
Finally, somewhat unique among the reconstructions discussed so far is the structure of the human SF3b

complex (~450 kDa) [40], a component of the U2 small nuclear ribonucleoprotein. Rather than using traditional cryo-EM, this structure was solved using cryo-negative stain. Although the staining process generally makes the evaluation of resolution difficult to interpret in comparison to pure cryo-EM structures, some helices are clearly visible in the structure and several structural motifs are unambiguously identified. This raises the possibility that such hybrid techniques may be useful at higher resolutions than previously believed possible.

Resolution, resolvability and model bias

When comparing several single-particle reconstruction publications side by side, it is immediately clear that there is considerable disparity in the resolutions quoted for structures with comparable levels of detail. Although this is true, this issue should not distract the scientific community from the broader perspective that, irrespective of the numerical resolution we assign to a particular structure, this technique is providing answers to important biological questions. Published structures are generally filtered to

Figure 4



A 6 Å resolution single-particle reconstruction of GroEL [30^{**}]. **(a)** The single-particle reconstruction thresholded such that α helices and β sheets can both be visualized. **(b)** The equatorial domain of the single-particle reconstruction with docked crystal structure (α helices, green; β sheets, blue) (PDB code 1OEL). **(c)** The equatorial domain of the 1OEL structure blurred to match the single-particle reconstruction. Arrow 1 indicates density observed in the single-particle reconstruction at the C terminus, where 23 residues are missing from the crystal structure. Arrow 2 indicates a bridge between helices observed in the single-particle reconstruction that is also observed in the crystal structure at this threshold.

make the highest level of reliable detail visible without introducing excess noise. So, irrespective of the specific numerical resolution, visual representations of reconstructions can generally be safely interpreted.

Of course, these numerical resolution values are considered important within the cryo-EM field because they act as a benchmark for those attempting to improve the technology itself and will become increasingly important as single-particle reconstruction approaches the resolutions obtainable using X-ray crystallography. Many of the proposed criteria are designed specifically to put cryo-EM and X-ray crystallography on a level playing field, for example [26]. However, some hold the alternative view that resolution should be directly related to the resolvability of the structure, and that an 8 Å resolution single-particle reconstruction must look similar to a crystal structure blurred with a Gaussian to 8 Å. Direct quality

comparisons between electron density maps produced by crystallography and single-particle cryo-EM are difficult, as the source of error at the limiting resolution in each case is very different. In single-particle cryo-EM, resolution is limited by the high noise level present in the particle images. In crystallography, phase determination and data incompleteness are the primary limiting factors. When single-particle cryo-EM is capable of producing atomistic reconstructions, this will provide a common basis for comparison with crystallographic reconstructions. Both sides of this argument make valid points, and there have been numerous different criteria and thresholds proposed over the years (see [41^{*},42], which include summaries of the various proposed criteria).

Although the details of these arguments are beyond the scope of a short review, it is important to note that all of the resolution criteria used in single-particle reconstruc-

tion are effectively measures of the noise level present in a reconstruction as a function of resolution. Current criteria do not measure the resolvability of the reconstruction and, in fact, arbitrary radial linear filters can be applied to a reconstruction (e.g. Gaussian high-pass or low-pass filters) without having any impact on the assessed resolution. Ideally, the resolvability of structures would be adjusted to match their measured resolution, but this cannot always be done in a straightforward manner. An additional complication is that initial model bias [43] and/or improper masking or averaging in the reconstruction can cause all of the resolution criteria to produce exaggerated resolutions. In short, precise resolution assessment remains an open issue. As a general guide for interpreting single-particle reconstructions: at subnanometer resolution, at least some α helices should be resolved; as resolution approaches 5 Å, helices should be clear and β sheets should be easily distinguished from helices; at some point beyond 5 Å resolution, it is expected that it will be possible to unambiguously trace the entire protein backbone.

Conclusions

Cryo-EM and single-particle reconstruction clearly have a bright future. The ability of this technique to address structural questions in a near-native environment, rather than being subjected to crystal packing forces, will lead to an increasing role in investigating structure/function relationships and dynamics. Microscope advances, such as improvements to stage stability, liquid helium cooled stages, better CCD cameras and inclusion of energy filters, are gradually improving image quality. Progress in software, automation and computational resources is increasing throughput. Over the next five years, we can expect that resolutions approaching 5 Å will be achieved and that subnanometer structures will become routine.

Update

The structure of skeletal muscle Ca^{2+} release channel (~2250 kDa) has recently been published at 9.6 Å resolution [44]. This represents the first structure of a membrane protein solved to subnanometer resolution using single-particle analysis. The structure permitted the identification of the pore-lining and pore-associated α helices in the channel; these were found to be very similar to the corresponding helices in the MthK potassium channel, raising some controversy about the mechanism of opening in both channels.

References and recommended reading

Papers of particular interest, published within the annual period of review, have been highlighted as:

- of special interest
- of outstanding interest

1. Bottcher B, Wynne SA, Crowther RA: **Determination of the fold of the core protein of hepatitis B virus by electron cryomicroscopy.** *Nature* 1997, **386**:88-91.
2. Conway JF, Cheng N, Zlotnick A, Wingfield PT, Stahl SJ, Steven AC: **Visualization of a 4-helix bundle in the hepatitis B virus capsid by cryo-electron microscopy.** *Nature* 1997, **386**:91-94.
3. Xiao C, Tuthill TJ, Bator Kelly CM, Challinor LJ, Chipman PR, Killington RA, Rowlands DJ, Craig A, Rossmann MG: **Discrimination among rhinovirus serotypes for a variant ICAM-1 receptor molecule.** *J Virol* 2004, **78**:10034-10044.
The structures of several variants of rhinoviruses and their cellular receptors were determined to around 10 Å resolution using cryo-EM. By fitting the crystal structures of both virus capsid and the receptor, detailed analysis of the binding sites was performed, revealing the mechanisms of differential binding characteristics.
4. Saban SD, Nepomuceno RR, Gritton LD, Nemerow GR, Stewart PL: **CryoEM structure at 9 Å resolution of an adenovirus vector targeted to hematopoietic cells.** *J Mol Biol* 2005, **349**:526-537.
5. Fabry CM, Rosa-Calatrava M, Conway JF, Zubieta C, Cusack S, Ruigrok RW, Schoehn G: **A quasi-atomic model of human adenovirus type 5 capsid.** *EMBO J* 2005, **24**:1645-1654.
6. Zhou ZH, Dougherty M, Jakana J, He J, Rixon FJ, Chiu W: **Seeing the herpesvirus capsid at 8.5 Å.** *Science* 2000, **288**:877-880.
7. Zhou ZH, Zhang H, Jakana J, Lu XY, Zhang JQ: **Cytoplasmic polyhedrosis virus structure at 8 Å by electron cryomicroscopy: structural basis of capsid stability and mRNA processing regulation.** *Structure* 2003, **11**:651-663.
8. Zhou ZH, Baker ML, Jiang W, Dougherty M, Jakana J, Dong G, Lu G, Chiu W: **Electron cryomicroscopy and bioinformatics suggest protein fold models for rice dwarf virus.** *Nat Struct Biol* 2001, **8**:868-873.
9. Zhang X, Walker SB, Chipman PR, Nibert ML, Baker TS: **Reovirus polymerase lambda 3 localized by cryo-electron microscopy of virions at a resolution of 7.6 Å.** *Nat Struct Biol* 2003, **10**:1011-1018.
Icosahedral reconstruction of the reovirus structure was mined to localize the embedded polymerase by fitting the crystal structures of all components. This is an example of deriving non-icosahedral component information for an icosahedral virus.
10. Mancini EJ, Clarke M, Gowen BE, Rutten T, Fuller SD: **Cryo-electron microscopy reveals the functional organization of an enveloped virus, Semliki Forest virus.** *Mol Cell* 2000, **5**:255-266.
11. Zhang W, Chipman PR, Corver J, Johnson PR, Zhang Y, Mukhopadhyay S, Baker TS, Strauss JH, Rossmann MG, Kuhn RJ: **Visualization of membrane protein domains by cryo-electron microscopy of dengue virus.** *Nat Struct Biol* 2003, **10**:907-912.
12. Huiskonen JT, Kivela HM, Bamford DH, Butcher SJ: **The PM2 virion has a novel organization with an internal membrane and pentameric receptor binding spikes.** *Nat Struct Mol Biol* 2004, **11**:850-856.
13. Jiang W, Li Z, Zhang Z, Baker ML, Prevelige PE Jr, Chiu W: **Coat protein fold and maturation transition of bacteriophage P22 seen at subnanometer resolutions.** *Nat Struct Biol* 2003, **10**:131-135.
Structures of phage P22 at the procapsid and mature phage stages were determined to subnanometer resolutions. This revealed, for the first time, the structural conservation of the major capsid protein fold among tailed dsDNA phages. Procapsid to mature phage maturation is now illustrated at the level of secondary structure element changes.
14. Morais MC, Choi KH, Koti JS, Chipman PR, Anderson DL, Rossmann MG: **Conservation of the capsid structure in tailed dsDNA bacteriophages: the pseudoatomic structure of phi29.** *Mol Cell* 2005, **18**:149-159.
The phage phi29 capsid structure was solved at 7.9 Å resolution. The major capsid protein was found to share a similar fold to phage HK97.
15. Wynne SA, Crowther RA, Leslie AG: **The crystal structure of the human hepatitis B virus capsid.** *Mol Cell* 1999, **3**:771-780.
16. Bowman BR, Baker ML, Rixon FJ, Chiu W, Quioco FA: **Structure of the herpesvirus major capsid protein.** *EMBO J* 2003, **22**:757-765.

The crystal structure of the upper domain of VP5 from herpes simplex virus validated the earlier cryo-EM structure of the capsid and the assignment of helices.

17. Nakagawa A, Miyazaki N, Taka J, Naitow H, Ogawa A, Fujimoto Z, Mizuno H, Higashi T, Watanabe Y, Omura T *et al.*: **The atomic structure of rice dwarf virus reveals the self-assembly mechanism of component proteins.** *Structure* 2003, **11**:1227-1238.
18. Fokine A, Leiman PG, Shneider MM, Ahvazi B, Boeshans KM, Steven AC, Black LW, Mesyanzhinov VV, Rossmann MG: **Structural and functional similarities between the capsid proteins of bacteriophages T4 and HK97 point to a common ancestry.** *Proc Natl Acad Sci USA* 2005, **102**:7163-7168.
19. Chapman MS, Liljas L: **Structural folds of viral proteins.** *Adv Protein Chem* 2003, **64**:125-196.
20. Benson SD, Bamford JK, Bamford DH, Burnett RM: **Does common architecture reveal a viral lineage spanning all three domains of life?** *Mol Cell* 2004, **16**:673-685.
21. Reinisch KM, Nibert ML, Harrison SC: **Structure of the reovirus core at 3.6 Å resolution.** *Nature* 2000, **404**:960-967.
22. Grimes JM, Burroughs JN, Gouet P, Diprose JM, Malby R, Zientara S, Mertens PP, Stuart DI: **The atomic structure of the bluetongue virus core.** *Nature* 1998, **395**:470-478.
23. Naitow H, Tang J, Canady M, Wickner RB, Johnson JE: **L-A virus at 3.4 Å resolution reveals particle architecture and mRNA decapping mechanism.** *Nat Struct Biol* 2002, **9**:725-728.
24. Heymann JB, Cheng N, Newcomb WW, Trus BL, Brown JC, Steven AC: **Dynamics of herpes simplex virus capsid maturation visualized by time-lapse cryo-electron microscopy.** *Nat Struct Biol* 2003, **10**:334-341.
25. Lata R, Conway JF, Cheng N, Duda RL, Hendrix RW, Wikoff WR, Johnson JE, Tsuruta H, Steven AC: **Maturation dynamics of a viral capsid: visualization of transitional intermediate states.** *Cell* 2000, **100**:253-263.
26. Rosenthal PB, Henderson R: **Optimal determination of particle orientation, absolute hand, and contrast loss in single-particle electron cryomicroscopy.** *J Mol Biol* 2003, **333**:721-745.
27. Borgnia MJ, Shi D, Zhang P, Milne JL: **Visualization of alpha-helical features in a density map constructed using 9 molecular images of the 1.8 MDa icosahedral core of pyruvate dehydrogenase.** *J Struct Biol* 2004, **147**:136-145.
28. Fotin A, Cheng Y, Sliz P, Grigorieff N, Harrison SC, Kirchhausen T, Walz T: **Molecular model for a complete clathrin lattice from electron cryomicroscopy.** *Nature* 2004, **432**:573-579.
An exceptional example of how subnanometer resolution structures should be presented. α Helices are clearly observed and larger motifs are identified.
29. Ranson NA, Farr GW, Roseman AM, Gowen B, Fenton WA, Horwich AL, Saibil HR: **ATP-bound states of GroEL captured by cryo-electron microscopy.** *Cell* 2001, **107**:869-879.
30. Ludtke SJ, Chen DH, Song JL, Chuang DT, Chiu W: **Seeing GroEL at 6 Å resolution by single particle electron cryomicroscopy.** *Structure* 2004, **12**:1129-1136.
The highest resolution single-particle reconstruction to date. This structure also demonstrates measurable differences between the crystal structure and the single-particle reconstruction.
31. Orlova EV, Gowen B, Droge A, Stiege A, Weise F, Lurz R, van Heel M, Tavares P: **Structure of a viral DNA gatekeeper at 10 Å resolution by cryo-electron microscopy.** *EMBO J* 2003, **22**:1255-1262.
32. Agirrezabala X, Martin-Benito J, Valle M, Gonzalez JM, Valencia A, Valpuesta JM, Carrasco JL: **Structure of the connector of bacteriophage T7 at 8 Å resolution: structural homologies of a basic component of a DNA translocating machinery.** *J Mol Biol* 2005, **347**:895-902.
The isolated T7 phage connector structure was solved by cryo-EM. The protein fold and the 12-fold symmetry are similar to that of the ϕ 29 phage connector crystal structure.
33. Simpson AA, Tao Y, Leiman PG, Badasso MO, He Y, Jardine PJ, Olson NH, Morais MC, Grimes S, Anderson DL *et al.*: **Structure of the bacteriophage phi29 DNA packaging motor.** *Nature* 2000, **408**:745-750.
34. Briggs JA, Huiskonen JT, Fernando KV, Gilbert RJ, Scotti P, Butcher SJ, Fuller SD: **Classification and three-dimensional reconstruction of unevenly distributed or symmetry mismatched features of icosahedral particles.** *J Struct Biol* 2005, **150**:332-339.
The authors demonstrate a method to solve the structure of non-icosahedral components of icosahedral particles. The method was applied to solve the structures of two different types of vertices of Kelp fly virus.
35. Morais MC, Tao Y, Olson NH, Grimes S, Jardine PJ, Anderson DL, Baker TS, Rossmann MG: **Cryoelectron-microscopy image reconstruction of symmetry mismatches in bacteriophage phi29.** *J Struct Biol* 2001, **135**:38-46.
36. Cheng Y, Zak O, Aisen P, Harrison SC, Walz T: **Structure of the human transferrin receptor-transferrin complex.** *Cell* 2004, **116**:565-576.
37. Matadeen R, Patwardhan A, Gowen B, Orlova EV, Pape T, Cuff M, Mueller F, Brimacombe R, van Heel M: **The Escherichia coli large ribosomal subunit at 7.5 Å resolution.** *Structure Fold Des* 1999, **7**:1575-1583.
38. Valle M, Zavialov A, Li W, Stagg SM, Sengupta J, Nielsen RC, Nissen P, Harvey SC, Ehrenberg M, Frank J: **Incorporation of aminoacyl-tRNA into the ribosome as seen by cryo-electron microscopy.** *Nat Struct Biol* 2003, **10**:899-906.
39. Menetret JF, Hegde RS, Heinrich SU, Chandramouli P, Ludtke SJ, Rapoport TA, Akey CW: **Architecture of the ribosome-channel complex derived from native membranes.** *J Mol Biol* 2005, **348**:445-457.
40. Golas MM, Sander B, Will CL, Luhmann R, Stark H: **Molecular architecture of the multiprotein splicing factor SF3b.** *Science* 2003, **300**:980-984.
41. Unser M, Sorzano CO, Thevenaz P, Jonic S, El-Bez C, De Carlo S, Conway JF, Trus BL: **Spectral signal-to-noise ratio and resolution assessment of 3D reconstructions.** *J Struct Biol* 2005, **149**:243-255.
In addition to proposing a new resolution criterion, the authors provide a good summary of the debate over resolution criteria.
42. Penczek PA: **Three-dimensional spectral signal-to-noise ratio for a class of reconstruction algorithms.** *J Struct Biol* 2002, **138**:34-46.
43. Stewart A, Grigorieff N: **Noise bias in the refinement of structures derived from single particles.** *Ultramicroscopy* 2004, **102**:67-84.
44. Ludtke SJ, Serysheva II, Hamilton SL, Chiu W: **The pore structure of the closed RyR1 channel.** *Structure* 2005, **13**:1203-1211.